Proceedings Paper:

Yan, Jiexiong, Dawson, John orcid.org/0000-0003-4537-9977 and Marvin, Andy orcid.org/0000-0003-2590-5335 (2018) Estimating reverberant electromagnetic fields in populated enclosures by using the diffusion model. In: Electromagnetic Compatibility (EMC), 2018 IEEE International Symposium on. 2018 IEEE International Symposium on Electromagnetic Compatibility (EMC), 30 Jul - 03 Aug 2018 IEEE EMC International Symposium . , USA , pp. 363-367.

https://doi.org/10.1109/EMCSI.2018.8495445

2018 IEEE International Symposium on Electromagnetic Compatibility (EMC)

Estimating reverberant electromagnetic fields in populated enclosures by using the diffusion model

Jiexiong Yan, John Dawson, *Member*, *IEEE*, and Andy Marvin, *Life Fellow*, *IEEE*
Department of Electronic Engineering
University of York
York, UK
{jy936, john.dawson, andy.marvin}@york.ac.uk

Abstract—**The ability of an enclosure to protect its contents from electromagnetic interference is quantified by its shielding effectiveness. Previous research has proved that the contents of an enclosure may greatly change the internal field and thus the shielding effectiveness. The power balance method is an efficient approach to analyze shielding problems of populated enclosures. One assumption of the power balance method is that in the steady state, the electromagnetic field in an enclosure is homogeneous. In actual circumstances, however, the presence of losses in an enclosure often compromises the field homogeneity and the power balance method may become inaccurate. A diffusion equation approach has been previously proposed to overcome this problem. In this paper, we predict the internal electromagnetic field of a populated enclosure by using the diffusion model, and compare them with the fields obtained by the power balance method, a full-wave electromagnetic solver and measurements, to demonstrate its efficacy. Comparisons between the diffusion model and the power balance method show that for populated enclosures, the internal electromagnetic field varies with position and that the diffusion model allows this to be observed.**

Keywords—diffusion model; reverberation chamber; shielding effectiveness

I. INTRODUCTION

In order to predict the shielding effectiveness of an enclosure, it is necessary to determine the electromagnetic field inside it. In real cases, an enclosure always has contents. Previous work has shown that the contents of an enclosure affect the shielding effectiveness because they absorb some energy and decrease the internal field [1]. The power balance (PWB) method has been widely used to study shielding problems of electrically large enclosures [2]. It stems from electromagnetic topology, dividing one big complex problem into several smaller and simpler ones [3]. For example, to a perforated and loaded enclosure, the internal energy loss consists of three parts: wall absorption, content absorption and aperture leakage. In this way, the walls and contents are characterized by their absorption cross sections (ACS) and the apertures are characterized by their transmission cross sections (TCS). The shielding effectiveness of the enclosure can then be calculated from the ACS and TCS [4]. The key feature of the PWB method is that it only considers average energy, so the detailed geometry of the contents is not required. Therefore, it takes much less computer resources than full wave solvers.

One of the basic assumptions of the PWB method is that in the steady state, the electromagnetic energy in an enclosure is completely diffuse and therefore uniformly distributed throughout the volume. This is true for low loss circumstances in which multiple reflections from enclosure walls lead to uniform and isotropic field. However, for moderate or high loss cases, the distribution of energy is no longer uniform and the PWB method does not account for this [5].

The acoustic community has proposed a diffusion equation based model that can account for the variation of the energy in an enclosure [6]. The diffusion model requires more computational resources than the PWB method, but still requires much less computational resources than full-wave solvers. Flintoft *et al* have shown that the diffusion model has the potential for electromagnetic applications such as shielding effectiveness [5]. However, the use of diffusion model assumes the enclosure to have a reverberant internal field and there is no guarantee that the results in [5] satisfy this condition. In order to further evaluate this method, we estimated the internal electromagnetic field of a populated enclosure by using the diffusion model and compared the results to full-wave simulation, reverberation chamber measurements and PWB method prediction. Section 2 outlines the theory of the diffusion model. Section 3 describes the details of the enclosure. Section 4 presents both diffusion and full-wave model of the enclosure. Section 5 gives the measurement methodology. Section 6 provides simulation and measurement results and Section 7 is the conclusion.

II. THE DIFFUSION MODEL

In [5], Flintoft *et al* have given a detailed review of the diffusion model. Here we only summarize the key points. The diffusion model compares the transport of electromagnetic wave in an enclosure to the transport of particles in a space. It assumes that there is a diffuse electromagnetic field with a time-averaged energy density at position r as

$$w(r) = \langle \frac{1}{2}[\varepsilon_0 E_t^2(r) + \mu_0 H_t^2(r)] \rangle \qquad (1)$$

where $E_t(r)$ and $H_t(r)$ are the total (rms) electric and magnetic fields; ε_0 and μ_0 are the vacuum permittivity and permeability. The symbol <·> means an average over a statistical ensemble of systems, for instance, due to mechanical or frequency stirring in a reverberation chamber. The diffuse electromagnetic energy

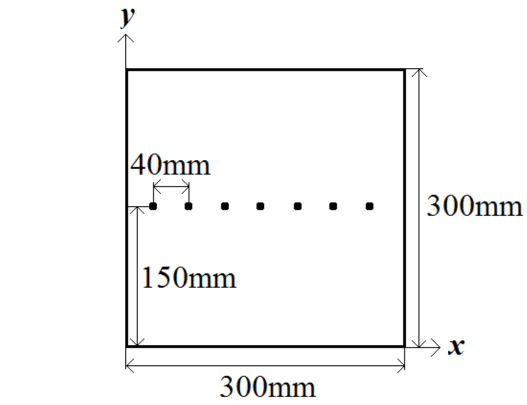

Fig. 1. Diagram of the lid of the enclosure, showing all seven measurement points. The aperture is at the center of the *x*=0 wall.

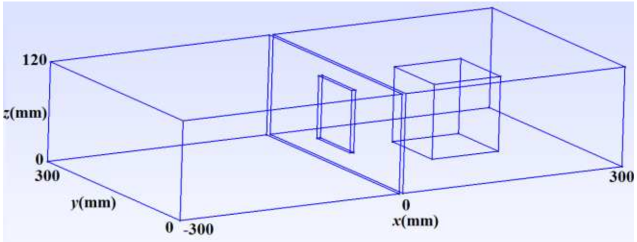

Fig. 2. The frame of the diffusion model. The cavity on the left side of *x*-axis represents a reverberation chamber and the one on the right side is the cavity we want to simulate. The two cavities are coupled by an aperture.

density in an enclosed space with a volume V satisfies the following diffusion equation

$$(D\nabla^2 + \Lambda)w(r) = P\delta^{(3)}(r - r_s) \quad (2)$$

where D is the diffusivity, Λ is volumetric energy loss rate from absorption in the enclosure contents and P is the total radiated power of a point source at position r_s. The diffusivity depends on the mean-free-path l between scatterings of rays in the space

$$D = \frac{lc}{3} \quad (3)$$

where c is the light speed. The energy loss rate from the absorption of contents is

$$\Lambda = \frac{c\alpha_{content}}{l_{content}} \quad (4)$$

where $\alpha_{content}$ is the absorption efficiency of the contents. The mean-free-path due to the walls and contents are given by equations (5) and (6) respectively.

$$l_{wall} = \frac{4V}{S_{wall}} \quad (5)$$

$$l_{content} = \frac{4V}{S_{content}} \quad (6)$$

where S_{wall} and $S_{content}$ are the surface area of the walls and contents respectively. The overall mean-free-path is the harmonic mean of all paths.

$$\frac{1}{l} = \frac{1}{l_{wall}} + \frac{1}{l_{content}} \quad (7)$$

On the boundary of the space, the energy density satisfies the Robin boundary condition

$$[D\hat{n} \cdot \nabla + c\,\Sigma_\alpha(r)]w(r) = 0 \quad (8)$$

where $\hat{n}$ is the outward unit normal vector and $\Sigma_\alpha(r)$ is the absorption factor. The simplest estimation of $\Sigma_\alpha(r)$ for the walls is Sabine's formula [7]

$$\Sigma_\alpha(r) = \frac{\alpha_{wall}(r)}{4} \quad (9)$$

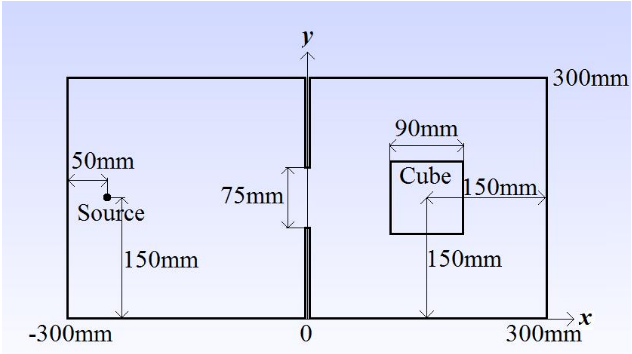

Fig. 3. Cross-sectional top view of the diffusion model at half height (*z*=60mm) showing the cube and the aperture. The left half is the reverberation chamber model, containing the source, used for the diffusion calculation.

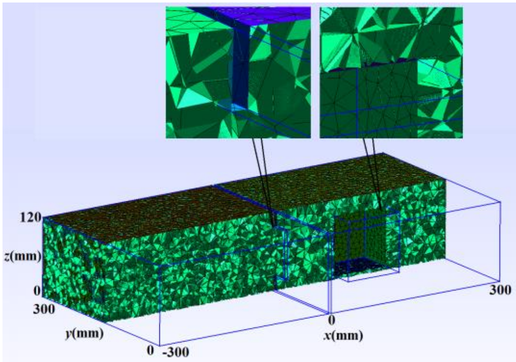

Fig. 4. Cross-sectional view of the 3D mesh of the diffusion model of the enclosure under test and source cavity; the two cavities can be seen, along with the aperture in the dividing wall and a void is seen in the location of the cube.

where $\alpha_{wall}(r)$ is the absorption efficiency of the walls.

The diffusion model is a generalization of the PWB method. When the energy in a space is static and uniform, the diffusion model reduces to the power balance model in [2]

$$(\sigma_{wall} + \sigma_{content})S^d_{enclosure} = P \quad (10)$$

where $S^d_{enclosure}$ is the power density in the enclosure; σ_{wall} and $\sigma_{content}$ are the absorption cross sections of the walls and contents respectively. Absorption cross section and absorption efficiency are related by

$$\sigma_{wall} = \frac{\alpha_{wall}S_{wall}}{4} \quad (11)$$

$$\sigma_{content} = \frac{\alpha_{content}S_{content}}{4} \quad (12)$$

By using the diffusion model, the shielding effectiveness of an enclosure is simply the ratio of power density in the absence and presence of the enclosure.

$$SE = \frac{S^d_0}{S^d_{enclosure}} \quad (13)$$

where S^d_0 is the power density without the enclosure.

III. Test Objects

The enclosure used in the simulation and measurements has dimensions of 300mm (length) ×300mm (width) ×120mm

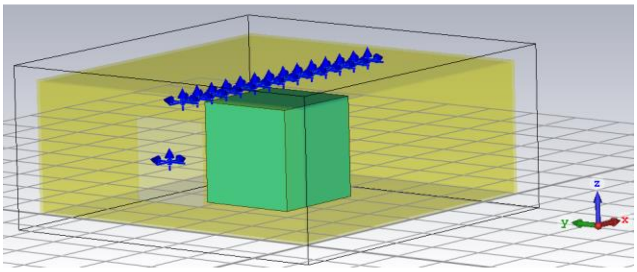

Fig. 5. Full-wave model of the enclosure under test showing the probes.

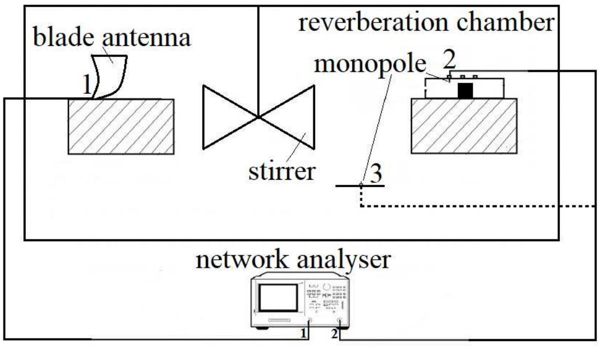

Fig. 6. Diagram of the validation measurement set up.

(height). There is a 75mm×75mm aperture at the center of the front panel. The lid of the enclosure is removable to allow access and there are seven positions in which a monopole can be installed. These are distributed along the central line of the lid at intervals of 40mm as shown in Figure 1. The enclosure is made from the same material as that in [5] and is assumed have the same absorption efficiency of α_{wall} =0.0027.

An absorbing cube with sides of length 90mm was put in the middle of the enclosure. It was made from the same LS22 radio absorbing material as the cylinder in [5] and is assumed have the same absorption efficiency of $\alpha_{content}$ =0.95. The DC conductivity of LS22 is 0.1mS/m according to Table 1 in [8].

IV. Simulation

A. Diffusion model

We follow Flintoft *et al* in using the FreeFEM++ software to perform the simulation [9]. The enclosure and the cube were modelled by including their surfaces in the mesh and applying the boundary condition (8) with the proper absorption factor. In order to minimise the size of the FreeFEM++ model we represented the reveberation chamber by a second small volume adjcent to the first. Figure 2 shows the frame of the diffusion model. The cavity on the left side of x-axis represents a reverberation chamber and the one on the right side is the cavity we want to simulate. The two cavities are coupled by an aperture and their walls are assumed have the same abosrption efficiency. We used a single isotropic point source for the simulation and it is located in the space that represents the reveberation chamber. Figure 3 shows the cross section of the diffusion model at the half height (z=60mm) plane. It allows the point source and the aperture in the middle to be better observed. Figure 4 shows the 3D mesh of the diffusion model and the mesh was generated by using the Gmsh software [10].

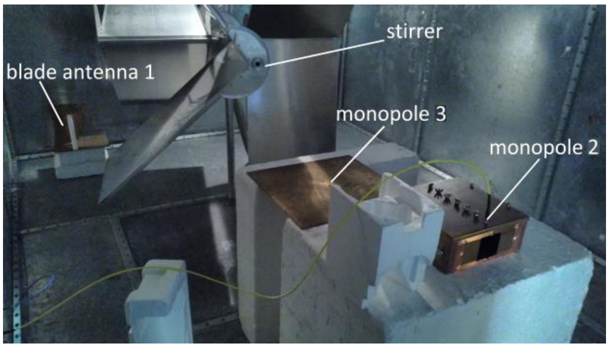

Fig. 7. Photograph of the validation measurement set up. The blade antenna 1 and monopoles 2, 3 are in accordance with those in Figure 6.

It can be noticed that the cube is represented by a hollow space. This is because the cube has a very high absorption efficiency and we assume that there is no energy penetration into it.

The energy density $w(r)$ in the enclosure is calculated by using the formulas detailed in section 2. It should be pointed out that the field in the vicinity of the point source can not be considered diffuse, so in the final results they should be discarded. When the energy density is obtained, the power density in the enclosure is

$$S^d_{enclosure} = cw(r) \tag{14}$$

The FreeFEM++ simulation finished in only a few seconds on a desktop computer (Intel Core i7-870 @ 2.93GHz, 8GB RAM).

B. Full-wave model

We used the CST Microwave Studio 2016 software to preform full-wave simulation [11]. Figure 5 shows the model of the enclosure and the cube. A line of probes was defined along the central line of the lid and they are in accordance with those in Figure 1. It can be noticed that there are more probe in the CST model than in the actual enclosure. This is because in the CST software, field probes are not physical and there is no coupling between them. Therefore, we could set the probes in CST closer together than in the actual measurements. An extra probe was set at the center of the aperture so that the energy of the power that enters the enclosure can be obtained. The probes record both electric and magnetic fields from 1GHz to 10GHz and the power density along the line can be calculated from

$$S^d_{enclosure} = \frac{1}{2}\left(\frac{|E_t|^2}{Z_0} + Z_0|H_t|^2\right) \tag{15}$$

where $Z_0 \approx 377\Omega$ is the free space impedance.

The diffuse environment in the CST simulation was created by using a number of ideal plane waves to illuminate the enclosure from different positions. We follow the Gauss-Legendre quadrature to choose the incident angles of the plane waves [12]. In [8], Flintoft *et al* stated that 32 incident directions (64 plane waves in total since to each direction there are two polarizations, vertical and horizontal) are sufficient to simulate a reverberant environment. Therefore in our simulation, we used 64 plane waves.

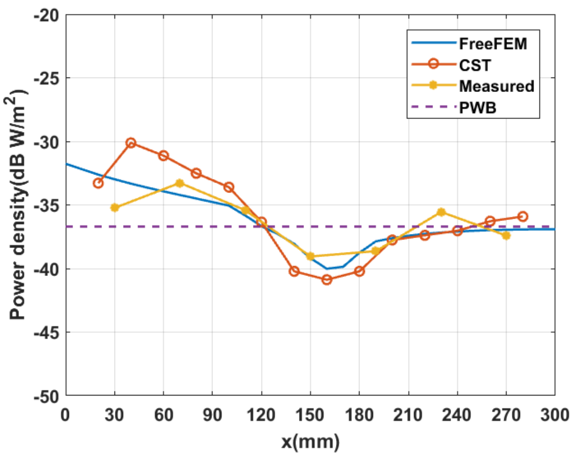

Fig. 8. Power density along the central line of the lid of the enclosure

V. VALIDATION MEASUREMENTS

The validation measurements of the enclosure were performed in a reverberation chamber with dimensions of 4.7m×3m×2.37m. Figure 6 shows the diagram of the measurements. We used the three-antenna method as recommended in IEEE Standard 299.1 [13]. Antenna 1 (the blade antenna) is the radiation source. Antenna 2 is a monopole that was fitted to the hole on the lid of the enclosure and antenna 3 is another similar monopole that was fitted onto a metal plane with the size of 480mm×480mm. The reverberation chamber was tuned using a mechanical stirrer using 100 equally spaced stirrer positions in one rotation. A network analyzer first measured the S-parameters between antennas 1 and 2, then between antennas 1 and 3 from 1GHz to 10GHz with 10001 equally spaced points. Figure 7 shows the photo of the measurement configuration. The blade antenna 1, monopole 2, monopole 3 and mechanical stirrer are in accordance with those in Figure 6. During the measurements, the unused holes on the enclosure lid were covered and the unused monopole (either antenna 2 or 3) was connected to a 50Ω load.

The mismatch corrected insertion gain between the transmitting and receiving antennas was calculated from the S-parameters [5]

$$IG_{1i} = \frac{\langle |S_{i1}|^2 \rangle}{(1-|\langle S_{11} \rangle|^2)-(1-|\langle S_{22} \rangle|^2)} \quad (16)$$

where i=2, 3. S_{21} and S_{31} are the transmission coefficients measured between the blade antenna 1 and monopole 2 and 3 respectively; S_{11}, S_{22} and S_{33} are the reflection coefficients of the three antennas respectively. If the radiation source is continuous, then the power density is proportional to IG and can be estimated by

$$\frac{IG_{13}}{IG_{12}} = \frac{S^d_{chamber}}{S^d_{enclosure}} \quad (17)$$

where $S^d_{chamber}$ is the power density in the chamber.

VI. RESULTS

Figure 8 compares the power density obtained from the diffusion model, CST simulation, measurement and PWB method prediction along the central line of the lid of the enclosure. It should be pointed out that in order to make the comparison, to the measurement, full-wave simulation and the diffusion model, the power that enters the enclosure should the same density.

In the CST simulation, the electric field strength of the plane wave is 1V/m. According to (15), the density of the input power is approximately 1×10^{-3} W/m^2. In order to compare the results obtained from FreeFEM++ and from CST simulation, it is necessary to normalize the density of the input power in the FreeFEM++ model to the same value. This was achieved by setting the radiated power P in (2) to 2×10^{-6}W to make the power density in the aperture area (x=0 plane) close to 1×10^{-3} W/m^2.

As for the measurement, the power density in the reverberation chamber, $S^d_{chamber}$ in (16), was also set as 1×10^{-3} W/m^2. It should be pointed out that to the CST simulation and measurements, we show the power density at the center frequency, which is 5.5GHz. Because the first resonant frequency of the enclosure is 700MHz and as a rule of thumb, the lowest usable frequency of an enclosure is three times the first resonant frequency [14]. Therefore at 5.5GHz we assume a diffuse field has been established. It can be seen that the diffusion model, CST simulation and measurement produced similar results. Although they are not identical, the general trends are the same. In the middle of the enclosure, the power density is lower than those in other positions. This is expected due to the presence of the absorbing cube. The PWB prediction was obtained from (10) and produced a constant value. As has been mentioned, this is due to the fact that it assumes in the steady state, the energy is uniformly distributed in the enclosure.

VII. CONCLUSION

The diffusion equation based model is a generalization of the already widely used PWB method for electrically large enclosures. It is able to account for the inhomogeneous electromagnetic field, which results from, for example, uneven distribution of contents in an enclosure. This feature is particularly useful in predicting shielding effectiveness of loaded enclosures like electronic devices, enabling the optimal positioning of contents to minimize the systematic error due to the loading. Another important feature of the diffusion model is its efficiency. It gives a solution in just seconds on a desktop computer, which allows fast estimations of shielding effectiveness to be undertaken at early stages of EMC design.

In this paper we demonstrated the efficacy of the diffusion model by predicting the power density in a loaded enclosure and comparing the results with those obtained by full wave solver, measurements and PWB prediction. Due to the limited capacity of the desktop computer, the simulations only went up to 10GHz. The comparison shows the agreements between the predictions of diffusion model, full-wave model and measurements are good. They all show the variation of the power density with position. The PWB method, on the other hand, predicts a constant value. The difference between our measurements and those in [5] is that ours were performed in a reverberation chamber and therefore a reverberant electromagnetic environment was guaranteed.

Extensions to this work include investigating the effect of apertures on the diffuse field since the presence of apertures might change the mean-free-path of walls and affect the local diffusivity. Another problem is that to a volume with a large spacing ratio (one dimension is much larger than the other one), the diffusivity may not be constant. It is necessary to predict the change of diffusivity along the longest dimension in order to obtain accuracy solutions. Solving these problems would enable the diffusion model to be applied to more complex structures.

REFERENCES

[1] A. C. Marvin, J. F. Dawson, S. Ward, L. Dawson, J. Clegg and A.weissenfeld, "A proposed new definition and measurement of the shielding effect of equipment enclosures," IEEE Transcations on Electromagnetic Compatibility, vol. 46, no. 3, pp. 459-468, August 2004.

[2] D. A. Hill, M. T. Ma, A. R. Ondrejka, B. F. Riddle, M.L. Crawford and R. T. Johnk, "Aperture excitation of electrically large, lossy cavities," IEEE Transcations on Electromagnetic Compatibility, vol. 36, no. 3, pp. 169-178, August 1994.

[3] I. Junqua, J. P. Paramantier and F. Issac, "A network formulation of the power balance method for high-frequency coupling," Electromagnetics, vol. 25, nos. 7-8, pp. 603-622, February 2005.

[4] I. D. Flintoft, S. L. Parker, S. J. Bale, A. C. Marvin, J. F. Dawson and M. P. Robinson, "Measured average absorption cross section of printed circuit boards from 2 to 20GHz," IEEE Transcations on Electromagnetic Compatibility, vol. 58, no. 2, pp. 553-560, April 2016.

[5] I. D Flintoft, A. C. Marvin, F. I. Funn, L. Dawson, X. Zhang, M. P. Robinson and J. F. Dawson, "Evaluation of the diffusion euqation foe modelling reverberant elecrromagnetic fields," IEEE Transcations on Electromagnetic Compatibility, vol. 59, no. 3, pp. 760-769, June 2017.

[6] L. Savioja And U. P. Svensson, "Overview of geometrical room acoustic modeling techniques," The Journal of the Acoustical Society of America, vol. 138, no. 2, pp. 708-730, August 2015.

[7] W. C. Sabine, Collected papers on acoustics, Harvard University Press, Cambridge, USA, 1922.

[8] I. D. Flintoft, S. J. Bale, A. C. Marvin, M. Ye, J. F. Dawson, C. Wang, M. Zhang, S. L. Parker and M. P. Robinson, "Representative contents design for shielding enclosure qualification from 2 to 20GHz," IEEE Transcations on Electromagnetic Compatibility, vol. 60, no. 1, pp. 173-181, February 2018.

[9] F. Hecht, "New developments in FreeFEM++," Jooural of Numerical Methematics, vol. 20, no3. 3-4, pp. 251-265, December 2012.

[10] C. Geuzaine and J. F. Remacle, "Gmsh: a three-dimensional finite element mesh generator with built-in pre- and post-processing facilities," International Journal for Numerical Methods in Engineering, vol. 79, no. 11, pp. 1309-1331, May 2009.

[11] Microwave Studio. Computer simulation technology (CST). 2016. [online]. Available: https://www.cst.com.

[12] K. Atkinson, "Numerical integration on a sphere," Journal of the Australian Methemetical Society, Series B, vol. 23, pp. 332-347, 1982.

[13] Standard method of measuring the shielding effectivness of enclosured and boxes having all dimensions between 0.1m and 2m. IEEE Standard 299.1, Institute of Electrical and Electronics Engineers, Piscataway, NJ, USA, October 2013.

[14] A. K. Fall, P. Besnier, C. Lemoine, M. Zhadobov and R. Sauleau, "Determining the lowest usable frequency of a frequency-strrred reveberation chamber using modal density," Proceedings of the 2014 International Symposium on Electromagnetic Compatibility, pp. 263-268, September 2014.